ELSEVIER

Journal of Chromatography A, 691 (1995) 301–315

JOURNAL OF CHROMATOGRAPHY A

Sensitivity and selectivity of the electrochemical detection of the copper(II) complexes of bioactive peptides, and comparison to model studies by rotating ring-disc electrode

Jian-Ge Chen, Steven J. Woltman, Stephen G. Weber*

Department of Chemistry, University of Pittsburgh, Pittsburgh, PA 15260, USA

Abstract

Post-column reaction of peptides with Cu(II) can be used for the electrochemical detection of peptides as their biuret complexes. Understanding of the behavior (sensitivity at the anode and cathode in the dual-series electrochemical detector) of the system is facilitated through the observation of the rotating ring disc voltammetry of some model compounds. In operation, the anodic signal from the oxidation of the Cu(II)–peptide to the Cu(III) form can be used to detect peptides, or the downstream cathode can be used to detect the Cu(III) form. The signals appear at about 0.4 V (anode) for tetra- and longer peptides, 0.65 V for tripeptides. The anode signal is augmented by tyrosine (oxidation at 0.4–0.5 V) and tryptophan (0.5–0.6 V). If the cathode is used as the detector in a two working electrode cell, the sensitivity depends on the stability of the Cu(III) product. This is peptide dependent, but the signal is significant and useful analytically. Twenty-three bioactive peptides in two groups, naturally electrochemically active and naturally electrochemically silent, and several model compounds have been studied.

Both naturally electrochemically active peptides (contain tyrosine and/or tryptophan) and naturally electrochemically silent peptides have been studied. Chromatography with an acetonitrile gradient has been used to separate the peptides in each group. Detection limits are for non-electroactive peptides in the range of 16–100 fmol (10- μl injection 1.6–10 nM, 100 μl injection 0.16–1.0 nM), and for electroactive peptides in the range of 6–40 fmol (0.6–4.0 nM for a 10- μl injection and 60–400 pM for a 100- μl injection). A tryptic digest of bovine cytochrome c is easily seen at 100 nM.

1. Introduction

Peptides carry critical information in living systems [1]. Their quantitative determination represents a considerable challenge. Antibody-based binding assays are challenged by the homology of peptides that originate in the same propeptide or prepropeptide [2]. Reversed-phase liquid chromatography [3] and capillary electrophoresis [4] have the capability to separate peptides, but routine, commercially available detectors are often not capable of detecting at the concentrations required. Thus, separations methods are challenged by the detection problem.

For work around μM concentrations, a UV photometer or spectrophotometer at around 210 nm is a good detector. It has the advantage of being able to detect any peptide, for the absorbance transition on which it works is due to

* Corresponding author.

0021-9673/95/$09.50
SSDI 0021-9673(94)00843-4

the amide bond. Of course, many other species absorb at that wavelength, so selectivity is poor. For lower concentrations, fluorescence of derivatized peptides, e.g., *o*-phthalaldehyde (OPA) [5] and naphthalene-2,3-dicarboxaldehyde/CN (NDA) [6], have been successful. An optimized detector using an Ar^+ laser-based detector and a 150×1 mm reversed-phase column demonstrated a detection limit for OPA derivatives of sulfur-containing amino acids of about 10^{-10} *M* in 10 μl (1 fmol) [7]. The peptide derivatives do not yield as high a sensitivity as the amino acids because of differences in the photophysical properties of the isoindole derivatives [8]. These successful fluorescent reagents rely on the presence of the primary amine for their success. A significant fraction of peptides do not have primary amines, for example they may be cyclic, N-acylated, or pyroglutamate may be the amine terminus. Thus, while fluorescence derivatization has certainly established itself as a useful and robust approach, it will not permit detection of peptides without reactive amines.

We [9–11] have been developing electrochemical detection [12] with the goal of providing useful detection limits and universal applicability to peptides [9], especially those without electroactive functional groups, W (Trp) and Y (Tyr) [10,11]. We use the biuret reaction, in which basic copper tartrate reacts with the peptides, and then take advantage of the reversible electrochemistry of the Cu(II)/Cu(III) couple [9]. Peptides with Y and W are detectable without derivatization [13], however the reaction with Cu(II) leads to increases in sensitivity for Y- [14] and W- [15] containing peptides.

One of the goals in the overall development of this approach to detection is to understand and predict the sensitivity of the method to various peptides. There are two general issues. One is whether the peptides in which one is interested react with the Cu(II) and give a signal under useful conditions, while the other is whether there are particular conditions that allow for the detection of desired peptides with selectivity over other peptides. Incidentally, in contrast to the amine-reactive fluorescence reagents, the biuret reaction does not occur with amino acids. It is impossible to determine the detection properties of every peptide because of the number of them, and because of differences among peptides, it is not possible to generalize with certainty concerning individual peptides that carry a similarity. Nonetheless, we must, in order for the technique to be useful, provide some basis for understanding the above mentioned pair of issues. Our approach is to study model peptides by rotating ring-disc voltammetry [16], and to determine the detection properties of bioactive peptides independently. In this paper, the first using this approach, we have examined several bioactive peptides, and we have developed a core understanding for the basic electrochemistry of the Cu(II)–peptide complex. Each bioactive peptide has not been investigated in detail, so there are some results for which a satisfying chemical interpretation is not in hand. However, taken together, the results for the electrochemical detection of the bioactive peptides represents a survey that gives a broad feeling for the potential of the approach.

2. Experimental

2.1. HPLC with post-column reagent addition

We used reversed-phase chromatography (Hypersil C_{18}, 3 μm, 100×1 mm, Keystone Scientific, Bellefonte, PA, USA) with gradient elution (Waters 600 MS pump, Bedford, MA, USA). The binary gradient used as solvent A 0.1% trifluoroacetic acid (TFAA) (HPLC grade; Sigma, St. Louis, MO, USA), 3% 1-propanol (HPLC grade, Sigma) (except for the tryptic digest analysis); B was 0.1% TFAA, 3% 1-propanol (except for the tryptic digest analysis), 60% acetonitrile (HPLC grade; EM Science, Gibbstown, NJ, USA) in water. Timing details are provided in the figures. The post-column phase, 1.2 *M* carbonate buffer [0.6 *M* each of $NaHCO_3$ (Mallinckrodt, Paris, KY, USA) and Na_2CO_3 (Fisher, Pittsburgh, PA, USA)], pH 9.8, 3% 1-propanol (except for the tryptic digest analysis), copper sulfate (Fisher) at around m*M* (exact concentrations given in the figures), and sodium potassium tartrate (Fisher) at 6 times the Cu(II) concentration was pumped with an ISCO (Lincoln, NE, USA) syringe pump. The sodium

potassium tartrate used for HPLC was recrystallized from water. The temperature of both the post-column phase and the column were controlled. Typical volume flow-rates were column: 50 μl/min and post-column 20 μl/min. The post-column reactor was PTFE tubing that had been woven through a nylon net. Its volume was 105 μl which resulted in a reaction time of 1.5 min. All data in the tables have been obtained with 1.0 m*M* copper sulfate in the post-column reagent. Reagent sources are listed below.

2.2. Electrochemical detection

A BAS (W. Lafayette, IN, USA) Model LC-4C dual-electrode controller, and dual-series glassy carbon cell were used as the detector. The thermal equilibration unit, ordinarily positioned just before the cell, was removed from the system. Signals from the detector were acquired at 1 point/s by EZChrom (Scientific Software, San Ramon, CA, USA). Areas were determined after manually specifying the limits of integration for each peak. Noise measurements were made by picking a segment of baseline where there were no peaks, amplifying a 1-min section, taking the maximum signal in this window minus the minimum as the peak-to-peak noise, and dividing by 5 to estimate root mean square (rms) noise.

Bioactive peptides, cytochrome *c* and trypsin were all purchased from Sigma. All solutions were made in Milli-Q laboratory-deionized water, except N-formyl-MLFF (DMF), N-formyl-MLF, fibrinopeptide A, and ACTH 1–10 were prepared in 0.1 *M* acetic acid (Fisher), and octadecaneneuropeptides in 0.1 *M* NaOH (EM Science) solution. One-letter abbreviations are used for amino acids.

2.3. Tryptic digest

A 5.0-ml volume of a 2.0 mg/ml solution of bovine cytochrome *c* (Sigma) in 0.1 *M* pH 8.0 ammonium carbonate buffer was mixed with 5.0 ml of a 0.1 mg/ml solution of trypsin in the same buffer. The solution was incubated for 24 h at 37°C, and then frozen. Before injection, the solution was diluted by a factor of 810 to yield 100 n*M* injected protein.

2.4. Rotating ring-disc electrode (RRDE) studies

RRDE studies employed a DT-29 glassy carbon disc/glassy carbon ring electrode, ASR-2 rotator and RDE-3 potentiostat (all from Pine Instrument Co., Grove City, PA, USA). A platinum grid counter-electrode and Ag/AgCl (3 *M* NaCl) reference electrode were used. All potentials are reported relative to the reference electrode.

Peptides (GGG, GGGG, GGY, GYG, YGG, GGFL and YGGFL; all from Sigma), analytical-grade sodium hydroxide, boric acid and sodium hydrogencarbonate (Mallinckrodt), ACS-grade copper sulfate pentahydrate (Fisher), and ACS-grade disodium tartrate dihydrate (Baker, Phillipsburg, NJ, USA) were used without further purification.

Carbonate buffer, pH 9.80, was prepared by dissolving sodium hydroxide and sodium hydrogencarbonate to concentrations of 0.10 and 0.20 *M*, respectively; the pH was confirmed with a meter before use. Borate buffer, pH 10.0, was prepared by titration of 0.10 *M* boric acid/0.10 *M* KCl with solid sodium hydroxide. Copper–peptide solutions were prepared by first mixing peptide stock solution with copper sulfate solution. For copper–peptide (1:1) solutions, equimolar copper sulfate was used; otherwise, copper sulfate–tartrate (1:3) solution was mixed with peptide solution to give a peptide–copper–tartrate molar ratio of 1:5:15. Sufficient deionized water was then added to reach 10% of the final solution volume. Buffer was introduced to the solution initially dropwise with mixing, then rapidly after the characteristic color change indicated development of the complex.

RRDE data were collected with EZChrom chromatography software. Potentiostat voltage was switched on simultaneously with manual triggering of data collection. To plot hydrodynamic voltammograms, EZChrom files were converted to ASCII format using the data export utility, then processed with Stata statistical software (Computing Resource Center, Santa Monica, CA, USA).

In all RRDE experiments, the ring (collector) electrode was maintained at a potential of 0 mV. Background runs were performed in buffer for

copper–peptide (1:1) solutions, and in biuret reagent mixed with buffer for peptide solutions with excess copper. The background signal was found not to have rotation speed dependence at the potentials used. The electrode surface was conditioned before each run by wet polishing with 0.05-μm alumina, rinsing with a stream of deionized water, and then pretreating at a potential of 800 mV disc, 0 mV ring in carbonate buffer for 1 min.

To perform hydrodynamic voltammetry, the disc potential was swept linearly from 0 to 900 mV, using the sweep generator of the RDE-3 potentiostat. The usual sweep rate of 600 mV/min was reduced to 80 mV/min for the lowest rotation speed runs to preserve steady state electrochemical behavior.

Each rotation speed study was conducted with the disc maintained at a constant potential previously identified as being in limiting current regions based upon the voltammetry. In each run, the electrode was rotated initially at a constant moderate speed (500 to 1000 rpm) and then potential was applied to the disc. The non-faradaic charging current was allowed to decay for one min, then the rotation speed was varied manually in a random sequence. Data collected in the first minute were ignored. The rotation speed was maintained at each value long enough for the signal to stabilize; this ranged from a few seconds at the highest rotation speeds to tens of seconds at the lowest. Rotation speeds ranged from 15 to 10 000 rpm, with ten to fifteen different rotation speeds per run. The low speed pully of the ASR rotator was used at the low end of this range.

3. Results and discussion

3.1. Equivalence of time scales between RRDE and electrochemical detection

By comparison of mass transfer rates calculated from theory [16,17], we have found that the conditions used in the HPLC experiment correspond to low rotation speeds, on the order of 15 rpm. For detection at the higher flow-rates typical of larger columns, the correspondence occurs at higher rotation speeds. For example, at 3.0 ml/min and a 25-μm thick spacer in the electrochemical detector, the equivalent rotation speed is about 1000 rpm.

3.2. Peptide backbone by RRDE

A considerable body of work on the stability of, and kinetics and mechanism of the reactions of Cu(II)–peptide complexes exists [18]. We draw on this work heavily in the interpretation of the voltammetry of these compounds, which is much less investigated than the homogeneous chemistry of these compounds. Figs. 1 and 2 show representative anodic (disc) and cathodic (ring) voltammograms for the simple peptides GGG and GGGG. At high rotation velocities, the voltammogram of GGG shows a single wave at 0.67 V. The stability of the Cu(III)–GGG complex is evidenced by the large cathodic current. The theoretical maximum cathodic current as a fraction of the anodic current for our electrode pair is 0.37. This ratio, called the collection efficiency, N_{coll}, is 0.32 for GGG at 10 000 rpm. Comparison to the standard (GGGG at pH 11.6) shows that there is one electron transferred, as expected for the reaction Cu(II)–GGG$\rightarrow$Cu(III)–GGG. At lower rotation velocities there is a simultaneous increase in anodic current and decrease in cathodic current. This indicates an instability in the Cu(III)–GGG complex at this longer time. The products of the reaction that removes Cu(III) from the system are oxidized at the anode, leading to a higher current, and the depletion of the Cu(III) form of the complex leads to a reduction in cathodic current. Chemical studies on the stability of Cu(III)–peptides [19] indicates that the more α hydrogens a tripeptide has, the less stable the complex. Clearly GGG has the maximum number of α hydrogens, so it represents the minimum stability. Investigations of the peptides FGG, GFG, GGF have shown virtually identical behavior to GGG at the RRDE (data not shown).

GGGG (Fig. 2) shows two waves, more distinctly the higher the rotation velocity. The first

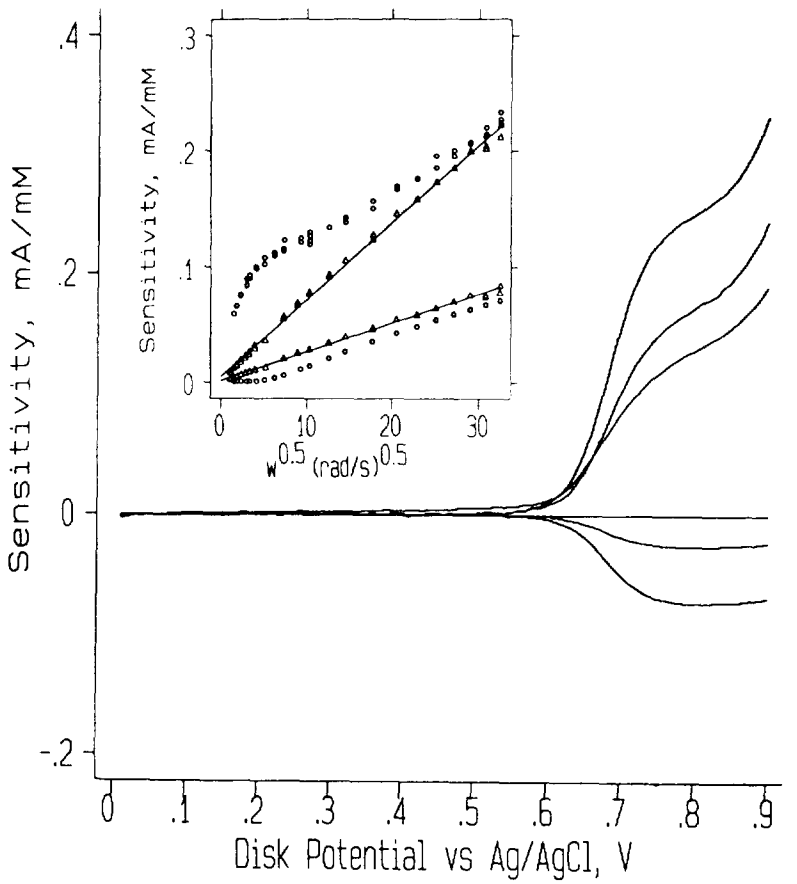

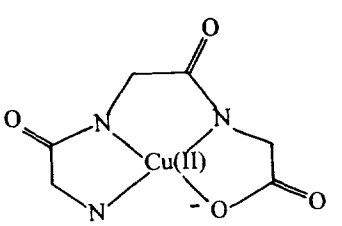

I

Fig. 1. RRDE voltammograms at pH 9.8 and structure of the Cu(II)–GGG complex. Anode (upward going) and cathode (downward going) traces are shown for (lowest to highest) 150, 2000, 10 000 rpm. In the inset is shown rotation speed dependent data for the anode at 0.7 V (upper set of points), and the cathode at 0.0 V (lower set of points). The cathode signal at the lowest rotation speed is negligible. The points associated with the regression lines are anode and cathode data for a standard one electron transferring species, Cu(II)–GGGG at pH 11.6.

wave at 0.42 V represents the more easily oxidized complex Cu(H_{-3}GGGG), shown in the figure as **II**. The negative subscript on H in the formula indicates that the loss of three protons from the neutral ligand was required to form the complex. The second wave at 0.67 V is from the Cu(H_{-2}GGGG) complex, **III**, which has around the Cu(II) the same atoms as the Cu(GGG)

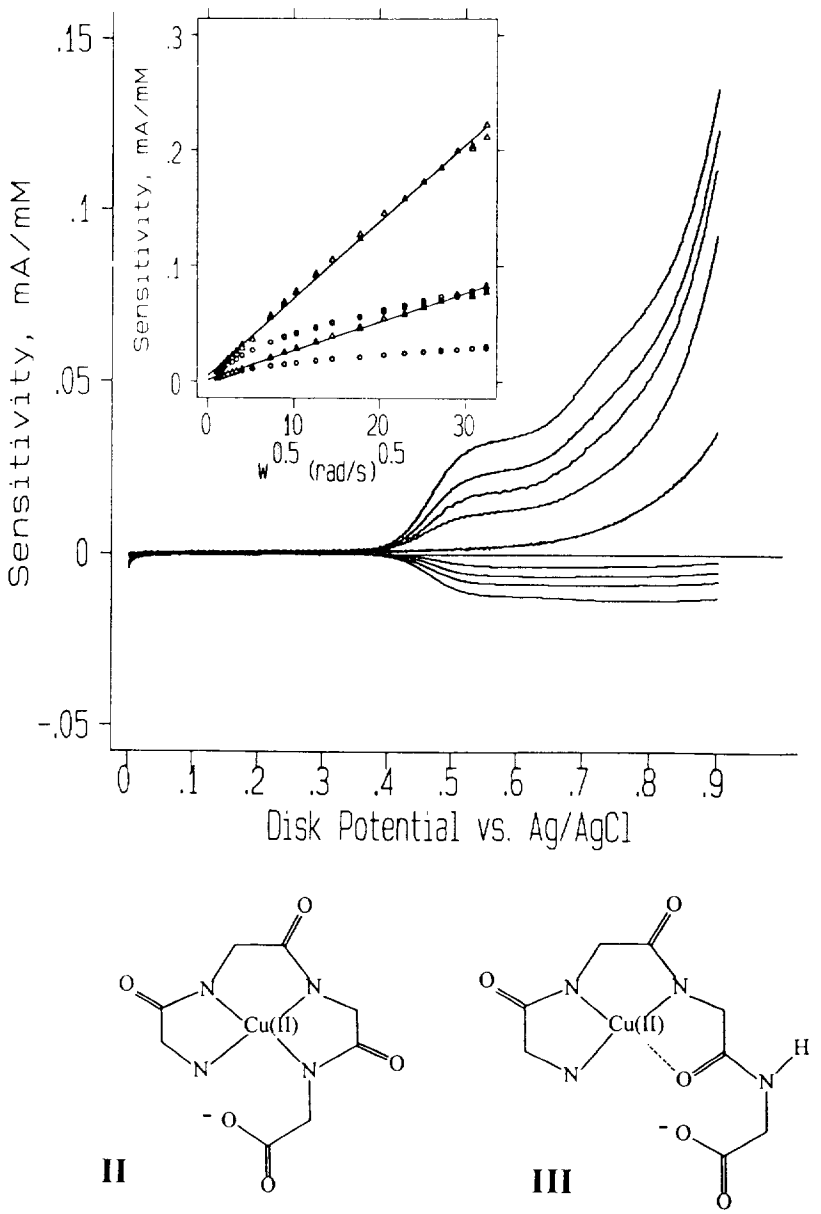

Fig. 2. RRDE voltammograms at pH 9.8 and structure of the Cu(II)–GGGG complex. Anode (upward going) and cathode (downward going) traces are shown for (lowest to highest) 15, 50, 100, 250 rpm plus anodic background (for all rotation speeds). The cathodic background is negligible. In the inset is shown rotation speed dependent data for the anode at 0.52 V (upper set of points), and the cathode at 0.0 V (lower set of points). The points associated with the regression lines are anode and cathode data for a standard one electron transferring species, Cu(II)–GGGG at pH 11.6.

complex (compare structures **III** and **I**). The near identity of the potentials is due to this homology. The appearance of two waves, with the second beginning to dominate the first, at higher rotation speeds is due to the slow interconversion between the H_{-3} and the H_{-2} forms of the complex [20]. Oxidation on the lower potential plateau removes Cu(II)(H_{-3}GGGG) from the solution, and by mass action the reaction:

Table 1
Sensitivities of small peptides at 0.55 and 0.80 V upstream anodic potentials and at 0.10 V of their corresponding downstream cathodic potentials (nC/pmol)

Peptide	Electrode potential (V)			
	0.55	0.10	0.80	0.10
GGF	0.14	0.00	54	0.82
GGFL	15	7.1	20	8.6
N-f-MLF	9.6	3.2	18	3.9
N-f-MLFF	2.4	0.61	2.5	1.2

$$\mathrm{Cu(II)(H_{-2}GGGG)} \rightarrow \mathrm{Cu(II)(H_{-3}GGGG)} \quad pK_a = 9.15 \qquad (1)$$

occurs. Thus, while the solution contains both forms, all of the complex can be oxidized at 0.55 V if the timescale is long enough. Of course, all of the complex is oxidized at 0.8 V, or at lower potentials and higher pH values; this reaction is not inhibited by homogeneous reaction kinetics. For both waves there is a substantial cathodic signal. A full study of the kinetics and mechanism of this electrochemical reaction is in progress. The equilibrium constant and rate constants for reaction 1 depend on the peptide, so the magnitude of the difference in anodic response depends on both the peptide and the time scale.

3.3. Electrochemical detection

First, the results discussed above will be used to understand the behavior of four small peptides. Following that, we will take a look at several peptide classes, and rationalize, where we can, the behavior based on the chemistry of the peptides.

Small peptides

Sensitivities for four small peptides may be found in Table 1. Of these, only two are "simple" peptides, two are N-formylated. The leu-enkephalin fragments, GGF and GGFL behave differently, as expected from the RRDE studies. At 0.8 V the signal from GGF exceeds that of GGFL by a factor of 2.7, while N_{coll} for GGFL is several-fold higher than for GGF. These results are qualitatively consistent with the RRDE studies. At 0.55 V the GGFL signal is somewhat lower, while that of GGF is significantly lower, again as expected from the RRDE work. As GGFL shows uncomplicated RRDE behavior that is in good qualitative agreement with the hydrodynamic voltammogram obtained by changing the potential at the electrochemical detector (Fig. 3), we accept that a sensitivity of about 20 nC/pmol represents a single electron transfer for a small peptide. Theory [17] predicts about 30 nC/pmol, however there are uncertainties in the actual diffusion coefficient, the actual

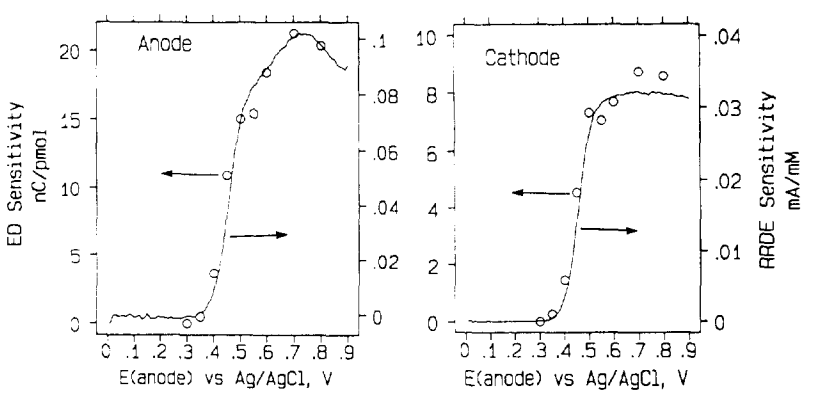

Fig. 3. Superimposition of RRDE voltammograms (solid line) and hydrodynamic voltammograms (HDV, O) from HPLC with electrochemical detection (ED). The vertical scales have been adjusted arbitrarily to give a fit pleasing to the eye.

cell thickness, nominally 12.5 μm, and in the actual velocity distribution across the channel, which is a full 6 mm wide. These uncertainties in the parameters that go into calculating the signal lead us to accept conditionally the experimental result, so we will use 20 nC/pmol as a benchmark for analysis of the results.

N-Blocked peptides

The N-formylated peptides react with the biuret reagent, but at 0.8 V only the N-f-MLF yields a signal approaching what would be expected for a straightforward one-electron transfer. Previous work on N-acetylated peptides [12] in flow injection analysis has pointed out the need for higher pH in the determination of these. Visible spectroscopic investigation of MLF, N-f-MLF, and N-acetyl-MLF at pH 9.8 (same as post-column reactor) shows that there is no formation of the N-acetyl-MLF complex, and partial formation of the N-f-MLF complex. Though a complete dependence study has not been carried out, we have noted that the sensitivity of the N-formylated peptides is very dependent on the Cu(II) concentration in the post-column reactor.

Another example of N-blocked peptides are those in which the amine terminal glutamate exists as the γ-lactam; this is pyroglutamate, pE. Table 2 compares sensitivities for substance P fragments pEFFGLM–NH_2, and QFFGLM–NH_2 (Q is Gln). They are very similar at both the cathode and the anode, and they are in the same range as the N-f peptides. We have established that the N-f and pE peptides are detectable, but further work to understand the reasons for the suppressed sensitivity is required.

Effect of peptide length

Data for a series of peptides are given in Table 2. Two of the peptides, lengths 4 and 8, show the full sensitivity that we expect. The other peptides (lengths 4, 6, 10, 13, 16, 18) show somewhat reduced sensitivity, but there is no distinct correlation with length. We can say, recalling the caveat about generalization stated above, that peptides up to 18 amino acids in length give acceptable signals. Lower sensitivity, where it occurs, is likely to be kinetic in origin, so reaction time, reaction temperature, and Cu(II) concentration can be used for improving the reaction rates.

Peptides with electroactive amino acids

At pH 9.8, Y is slightly easier to oxidize than W (0.56 vs. 0.67 V [21]). I is more easily oxidized than either. Neither W nor Y has a reversible redox wave, so we do not anticipate a useful cathode signal from peptides that have W and Y in the absence of Cu(II). In the presence of Cu(II), the anode signal may be the sum of the electroactive amino acid signal and the

Table 2
Sensitivites of non-electroactive bioactive peptides at 0.80 V upstream anode and 0.10 V downstream cathode (nC/pmol)

No.	Peptide	Amino acid sequence	Electrode potential (V)	
			0.80	0.10
1	RFDS	RFDS	14	6.4
2	Speract	GFDLNGGGVG	10	3.2
3	Des-Y-L-enkephalin	GGFL	20	8.6
4	Fibrinopeptide A	ADSGEGDFLAEGGGVR	14	5.1
5	Octadecaneuropeptide	QATVGDVNTDRPGLLDLK	7.51	2.2
6	N-Formyl-MLF	N-f-MLF	18	3.9
7	SPF 6–11[a]	QFFGLM–NH_2	8.7	2.3
8	pE[a]–SPF 6–11[a]	pEFFGLM–NH_2	5.8	2.8
9	ALILTLVS	ALILTLVS	21	9.3
10	HPPGRHF 14–26	DAENLIDSFQEIV	8.2	2.2
11	N-Formyl-MLFF	N-f-MLFF	2.5	0.46

[a] SPF = Substance P fragment.

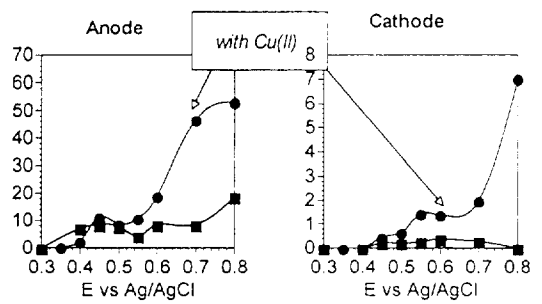

Fig. 4. HDV with and without Cu(II) for the tyrosine-containing peptide α-endorphin. Vertical scale nC/pmol. Lines are a cubic spine fit to the points. pH 9.8.

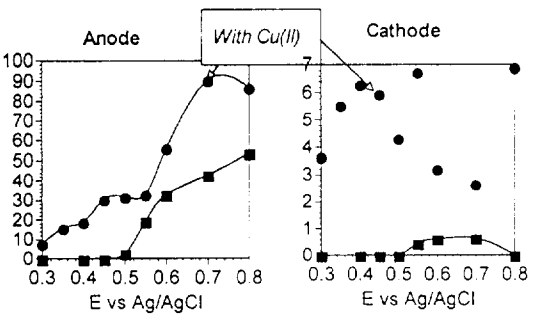

Fig. 5. HDV with and without Cu(II) for the tryptophan-containing peptide leucokinin II. Vertical scale nC/pmol. Lines are a cubic spine fit to the points. pH 9.8.

Cu(II) signal [14]. The cathode signal in this case is depressed in small Y-containing peptides [14]. Plots of the anodic and cathodic sensitivities as a function of potential at the anode are shown in Figs. 4 and 5 for representative peptides containing only W (leukokinin II, DPGFSSWG–NH_2) and only Y (α-endorphin, YGGFMTSEKSQTPLVT), and Table 3 gives sensitivities at the anode at 0.5 V and at the cathode (0.0 V) while the anode is at 0.8 V in the presence and absence of Cu(II) for several bioactive electroactive peptides. Before discussion we point out that the baseline at the cathode is more stable at 0.1 V, and sensitivities, where we have tested them, are the equivalent or higher than those at 0.0 V, however we have more complete data for more peptides at 0.0 V, thus we will concentrate on them. The increased baseline at 0.0 V is caused by the stabilizing influence of acetonitrile on Cu(I). As the acetonitrile content of the mobile phase increases, it becomes easier to reduce Cu(II) to Cu(I), and that reduction becomes background current.

The anodic voltammograms of the electroactive peptides without Cu(II) show behavior similar to that of model compounds (Figs. 6 and 7). In the absence of Cu(II), Y is more easily oxidized than W, the wave of YGGFL precedes that of GWGG, and the wave of the Y-con-

Table 3
Sensitivites of electroactive bioactive peptides at 0.50 and 0.0 V while the upstream anodic potential is at 0.80 V with (w/) and without (w/o) Cu^{2+} (nC/pmol)

No.	Peptide	Amino acid sequence	Electrode potential (V)			
			0.50 (w/)	0.00 (w/)	0.50 (w/o)	0.00 (w/o)
1	DSIP	WAGGDASGE	32	4.3	5.6	1.0
2	RKDVY	RKDVY	11	2.5	8.6	0.49
3	Lys^8-vasopressin	C(YFQN)CPLG–NH_2	36	1.6	20	0.71
4	Leucokinin II	DPGFSSWG–NH_2	32	6.9	2.9	0.0
5	Oxytocin	C(YIQN)CPLG–NH_2	40	3.1	9.5	0.21
6	Leu-enkephalin	YGGFL	60	10	21	0.58
7	WMDF-NH_2	WMDF-NH_2	29	7.3	8.2	1.0
8	Angiotensin II	DRVYIHPF	33	7.1	7.7	0.08
9	ACTH 1–10	SYSMEHFRWG	50	9.3	36	0.62
10	Neurotensin	pELYENKPRRPYIL	55	11	13	0.26
11	α-Endorphin	YGGFMTSEKSQTPLVT	56	8.3	36	2.3
12	Tyr-somatostatin	YAGC(KNFFWKTFTS)C	8.8	7.0	7.9	0.0

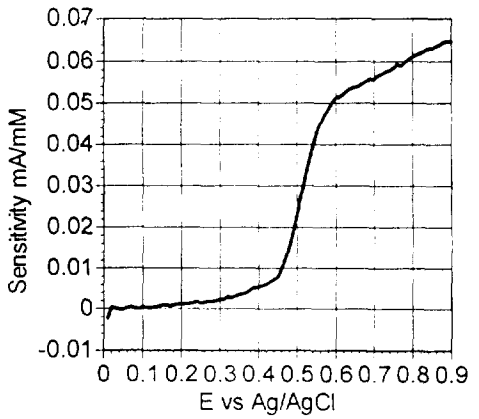

Fig. 6. RRDE voltammogram of YGGFL in the absence of Cu(II). pH 9.8.

taining α-endorphin is negative of that of the W-containing leucokinin II. The sensitivity suggests up to 2 electrons are transferred in the oxidation, which agrees with observations on the amino acids themselves. The cathode signals are lower than what is expected for a reversible reaction befitting the irreversible nature of the oxidations. The nominal two electron oxidation of Y- and W-containing peptides is most likely a sequence of reactions, an electron transfer followed by a chemical reaction, and then another electron transfer [14,15]. The rate of the chemical reaction dictates the lifetime of the first electron transfer product. This rate may certainly be peptide dependent, thus we may expect some peptides to give more significant cathodic signals than others as seen in Table 3. The examples shown in Figs. 4 and 5 represent extremes in this regard. The α-endorphin has a significant cathode signal, while that of the leukokinin II is zero.

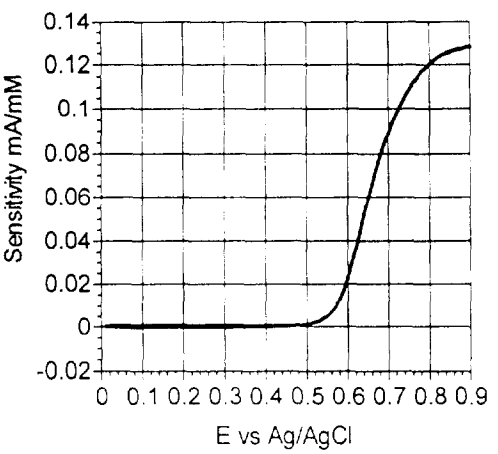

Fig. 7. RRDE voltammogram of GWGG in the absence of Cu(II). pH 9.8.

In the presence of the biuret reagent there is a considerable improvement in sensitivity, both at the anode at 0.5 V and at the cathode at 0.0 V (anode 0.8 V). The increase in sensitivity at 0.5 V is about 15–40 nC/pmol (Table 3) except for RKDVY and Y-somatostatin. Discussion of these is deferred. For the bulk of the peptides, the Cu chemistry expresses itself at a low potential as an additive factor. Furthermore, at the cathode, when the anode is at 0.8 V the sensitivities are the equal of those for typical non-electroactive peptides. This result is not the same as results for shorter peptides in which the cathode sensitivities are compromised by the presence of Y [14]. Let us consider the exceptions. The RKVDY will be discussed below, however for the somatostatin we must consider that the sensitivity of its detection without Cu is abnormally low (it contains W and Y) and its sensitivity at 0.5 V in the absence of Cu(II) is 7.9 nC/pmol. It may have a structure that inhibits electron transfer; it is highly basic. At 0.8 V, the sensitivity of the biuret complex of the Y-somatostatin is more normal. There is the possibility as well that the reaction analogous to reaction 1 above is slow, or the pK_a is very basic, which minimizes the H_{-3} wave and emphasizes the H_{-2} wave. This explanation, however, does not explain the low sensitivity to the Y and W in the peptide under Cu-free conditions.

Peptide structure

We have previously shown that bradykinin reacts slowly with the biuret reagent [10]. We rationalized this in terms of the limitations caused by proline on the accessible structures, which in turn limits the chance that the peptide is in an appropriate conformation to react with

Cu(II). Here, under different conditions of mobile phase, we have found the same result; anodic sensitivity (nC/pmol) is only 1.9 at 0.50 V and 0.39 for the corresponding cathode at 0.1 V. Substance P, which has 2 proline residues, appears to behave similarly; it only gives 0.72 and 0.14 nC/mol at the same applied potentials given for bradykinin.

Pre-column derivatization with Cu(II) was found to be an effective method for bradykinin [10]. A fuller study of highly constrained peptides is certainly warranted.

Many bioactive peptides are cyclic disulfides as a result of the formation of intramolecular S–S bridges by a pair of cysteines. Table 3 has data for Y-somatostatin, which has been discussed, and oxytocin and lys^{8}-vasopressin, all of which have cyclic, S–S bridged structures. A model RRDE voltammogram of CAAGVC is shown in Fig. 8. Clearly, this cyclical structure does not inhibit the formation of the complex. Once again, it is worth remembering the caveat concerning generalization, but at least one can say that the restrictions on structure due to the S–S bridge do not interfere with the detection of these peptides.

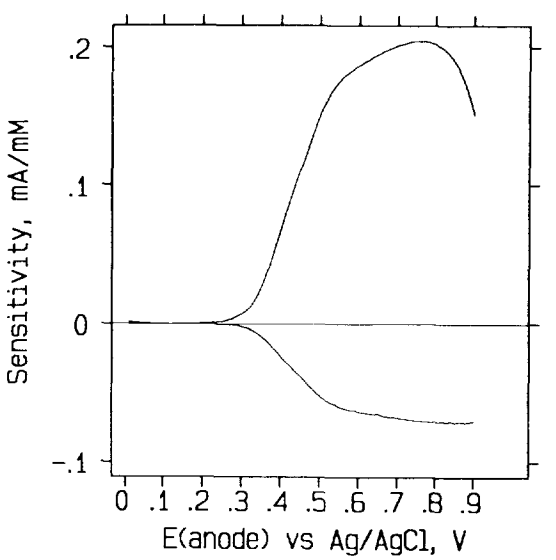

Fig. 8. RRDE voltammogram of CAAGVC at pH 9.8. 10 000 rpm.

RGD peptides are an important class of cell adhesion mediators [22]. It has been reported that the Cu(II) complexes of peptides with an aspartate in the third position from the amine terminus, which will be written as XXD, are very stable [23]. The stability arises because the β-carboxy group of the D is a ligand for the Cu(II); even in a tetrapeptide, the carboxy group is the fourth ligand in the complex, not the amide between the third and fourth amino acid. As we have seen above for the pair GGG and GGGG, the effect of the carboxy group on the electrochemistry is dramatic. Table 4 shows data from three peptides with the sequence XXDX.... Clearly the signal from Cu(II)–XXDX.. is low at 0.55 V, and higher at 0.8 V. This pattern reflects the chemistry of the tripeptide as expected for the purported structure of the complex. Though it has not yet been done, it can be predicted that these Cu(II) complexes will be stable even in mildly acidic conditions, and that rather selective detection of them at an anode will be possible because ordinary biuret complexes lose Cu(II) at such low pH values.

3.4. Example chromatograms

Fig. 9 shows the gradient separation of 100 μl of 50 n*M* non-electroactive peptides. The best signal-to-noise ratio comes from the cathode. The inserts show noise from two segments of the cathode voltammogram; the peak-to-peak noise is $6 \cdot 10^{-4}$–$8 \cdot 10^{-4}$ V, while the peak heights

Table 4
Sensitivities of XXDX.. peptides at 0.50 and 0.80 V (nC/pmol)

Peptide	Electrode potential (V)	
	0.50	0.80
RKDVY	11	57
RFDS	0.48	14
GFDLNGGGVG	0.24	10

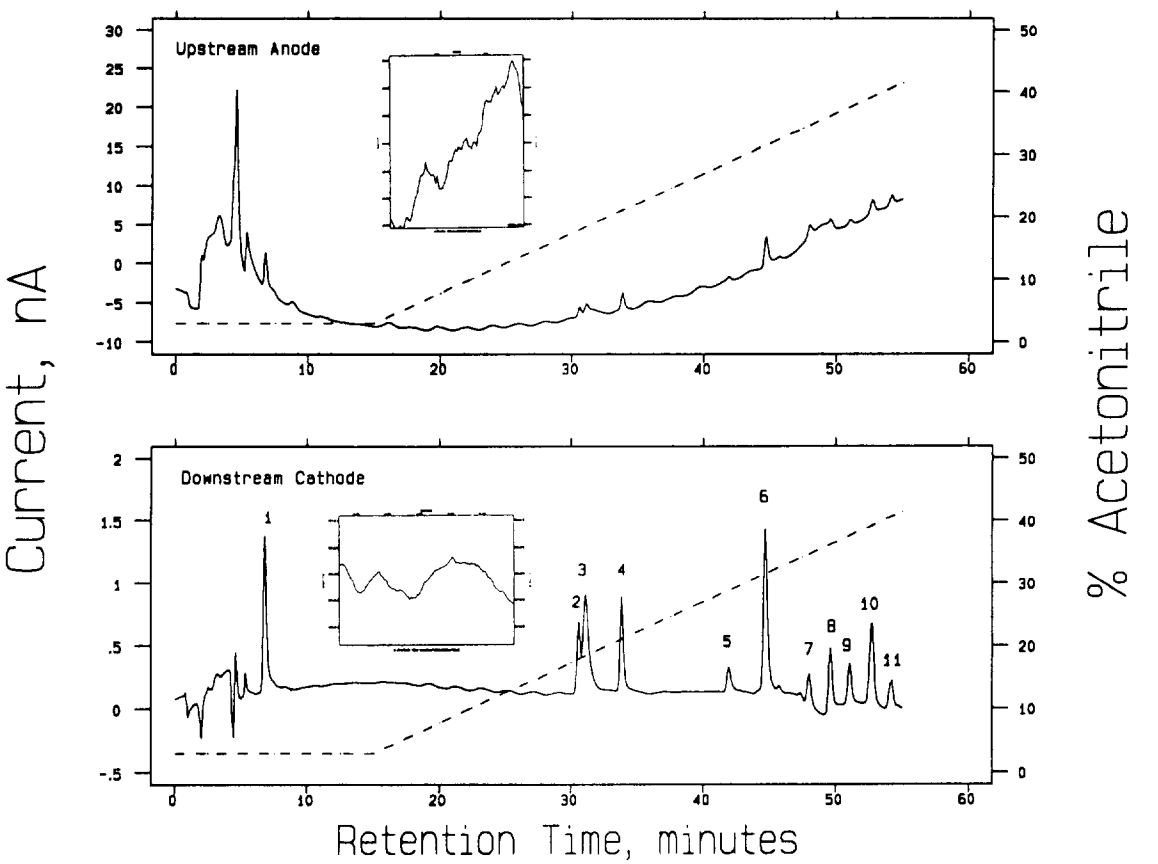

Fig. 9. Gradient elution chromatogram of the peptides in Table 2 (to which the numbers refer). Solvents A and B both have 0.1% TFAA and 3% 1-propanol; B also contains 60% acetonitrile. Gradient timing is shown with the dotted line. Post-column reagent: 0.5 m*M* Cu(II). Column and post-column temperatures 50°C. Upper chromatogram, anode 0.80 V, sensitivity 200 nA/V. Inset on upper, anode, trace is an expansion of the cathode trace's baseline at 40 min. It is 0.0006 V peak-to-peak. Lower chromatogram, cathode 0.09 V, sensitivity 10 nA/V. Inset is an expansion of the cathodic baseline at 38 min. It is 0.0008 V peak-to-peak.

range from about $2 \cdot 10^{-2}$ to 0.1 V. The signal to rms noise ratio is 3 when the signal is about $4 \cdot 10^{-4}$ V, which corresponds to the range of 20–100 fmol injected. Fig. 10 shows the anodic voltammogram (0.55 V) from the electroactive peptides. In this experiment, both electrodes were used as anodes at 0.55 V. The signal-to-noise ratio is better at the upstream electrode, ranging from 6–40 fmol injected. Table 5 shows linear regression results of calibration curves (0.5 V anode) for the electroactive peptides except for 1 and 2 which were not well-retained. Other than Tyr-somatostatin, which has been discussed and gives good sensitivity at 0.8 V, the curves are acceptable. It is hard to see in the curves, but there is some tendency among several peptides to lose sensitivity at low concentrations. This is undoubtedly due to adsorptive loss of the peptides which we have done nothing to prevent.

Fig. 11 shows the injection of 100 μl of 100 n*M* of a cytochrome *c* tryptic digest. Eleven peaks are expected; Fig. 11 shows clearly 10

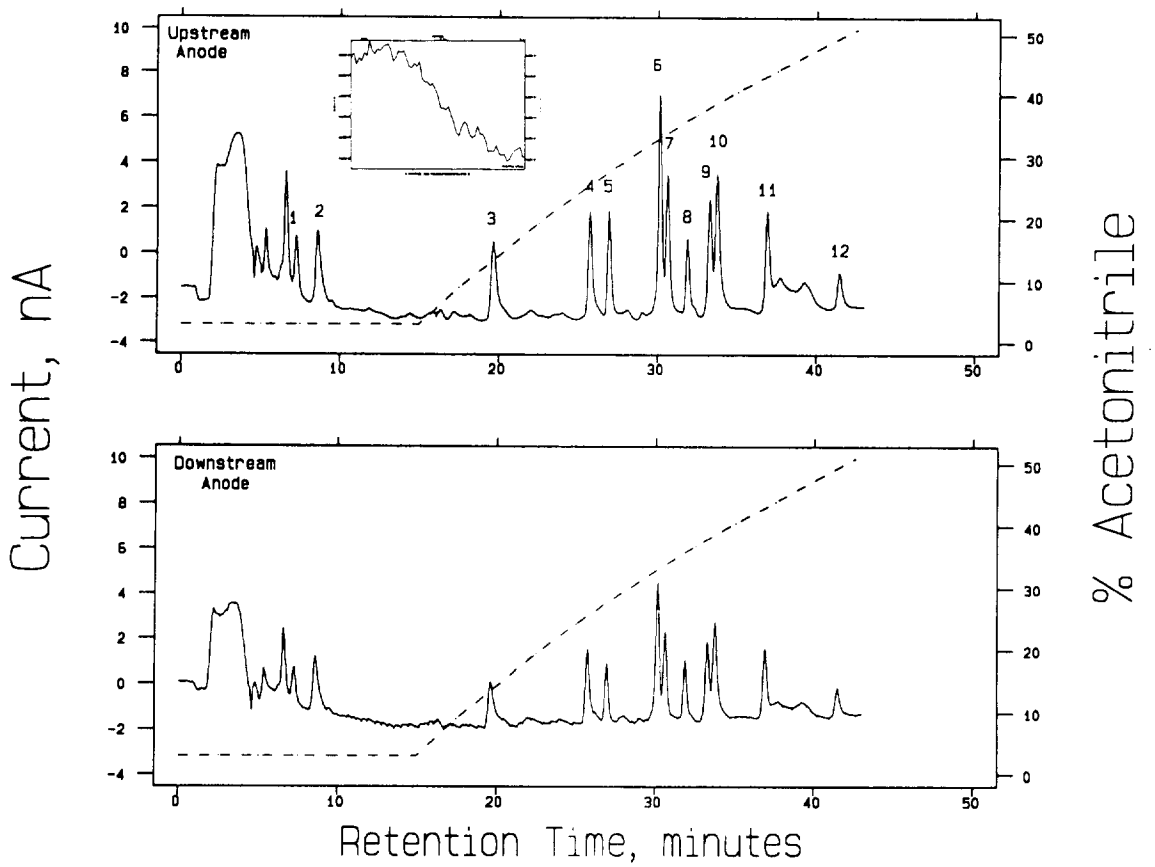

Fig. 10. Gradient elution chromatogram of the peptides in Table 3 (to which the numbers refer). Both solvents A and B have 0.1% TFAA and 3% 1-propanol; B also contains 60% acetonitrile. Gradient timing is shown with dotted line. Post-column reagent: 0.2 m*M* Cu(II). Column and post-column temperatures 50°C. Upper chromatogram, anode 0.55 V, sensitivity 100 nA/V. Inset on upper, anode, trace is an expansion of the anode trace's baseline at 11 min. It is 0.0005 V peak-to-peak. Lower chromatogram, also an anode at 0.55 V, sensitivity 100 nA/V.

Table 5
Linear regression results of some electroactive peptides obtained with an anodic applied potential of 0.55 V

Compound	Slope (nC/pmol)	*y*-Intercept (nC)	R^2
Lys^8-vasopressin	49	−4.7	0.995
Leucokinin II	36	1.6	0.985
Oxytocin	42	−3.2	0.999
Leu-enkephalin	88	−1.6	0.996
WMDF-NH_2	61	−5.1	0.999
Angiotensin II	32	−7.4	0.991
AHF 1–10	37	5.6	0.991
Neurotensin	72	−2.9	0.981
α-Endorphin	38	−9.1	0.997
Tyr-somatostatin	6.1	14	0.906

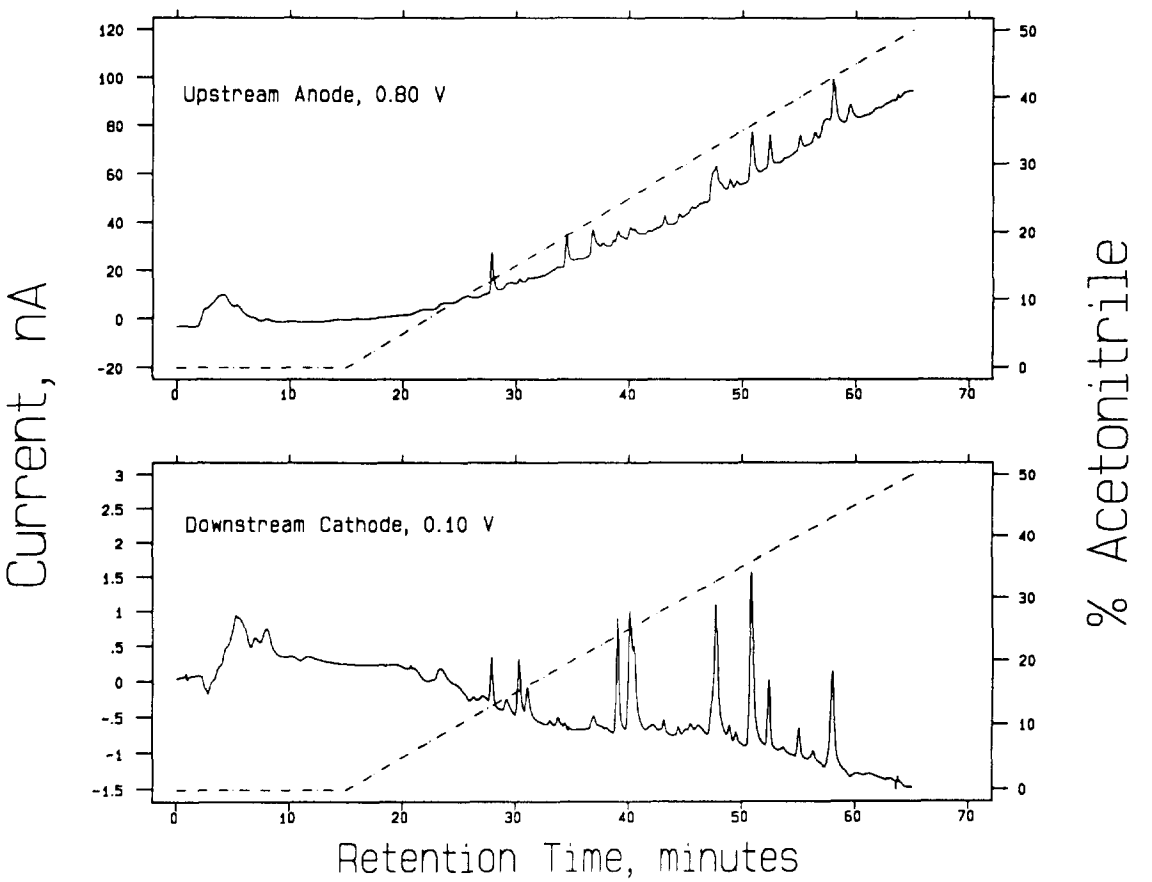

Fig. 11. Gradient elution of 100 n*M* tryptic digest fragments of cytochrome *c*. Both solvents A and B contain 0.1% TFAA; B also contains 3% 1-propanol and 60% acetonitrile. Gradient timing is shown with the dotted line. Post-column reagent: 0.5 m*M* Cu(II). Column and post-column temperatures 50°C. Top: anode at 0.8 V; bottom: Cathode at 0.10 V.

(cathode) one which, at about 48 min, is certainly a pair of peaks.

4. Conclusions

We have demonstrated the application of the biuret reaction for peptide detection with post-column reaction. Peptide sensitivities for electrochemical detection were predicted by model compound studies with the rotating ring-disc electrode. The Cu(II)–peptide electrochemistry of several classes of peptides has been characterized. The response of this detection technique was shown to be linear and to exhibit low detection limits for the oligopeptides studied, ranging from 0.16 to 4 n*M* for a 100-μl injection. Finally, the technique was applied to a tryptic digest of cytochrome *c*.

Acknowledgement

We are pleased to thank NIGMS for financial support through grant 44842.

References

[1] T. Hökfelt, *Neuron*, 7 (1991) 867.
[2] D. Liu, C. Dass, G. Wood and D.M. Desiderio, *J. Chromatogr.*, 500 (1990) 395.

[3] W.S. Hancock and D.R.K. Harding, in W.S. Hancock (Editor), *Handbook of HPLC for the Separation of Amino Acids, Peptides, and Proteins*, Vol. II, CRC Press, Boca Raton, FL, 1984, p. 3.
[4] J.R. Mazzeo and I.S. Krull, in N.A. Guzman (Editor), *Capillary Electrophoresis Technology*, Marcel Dekker, New York, 1993, p. 795.
[5] O. Orwar, S. Folestad, S. E. Einarsson, P. Andiné and M. Sandberg, *J. Chromatogr.*, 566 (1991) 39.
[6] R.G. Carlson, R.S. Srinivasachar and B.K. Matuszewski, *J. Org. Chem.*, 51 (1986) 3978.
[7] O. Orwar, M. Sandberg, M. Sundahl, S. Folestad and I. Jacobson, *Anal. Chem.*, in press.
[8] O. Orwar, M. Sandberg, S. Folestad, A. Tivesten, S.G. Weber and M. Sundahl, *J. Chromatogr.*, in press.
[9] A.M. Warner and S.G. Weber, *Anal. Chem.*, 61 (1989) 2664.
[10] H. Tsai and S.G. Weber, *J. Chromatogr.*, 542 (1991) 345.
[11] H. Tsai and S.G. Weber, *J. Chromatogr.*, 515 (1990) 451.
[12] L. Dou, J. Mazzeo and I.S. Krull, *BioChromatography*, 5 (1990) 74.
[13] L.H. Fleming and N.C. Reynolds, Jr., *J. Chromatogr.*, 431 (1988) 65.
[14] H. Tsai and S.G. Weber, *Anal. Chem.*, 64 (1992) 2897.
[15] H. Tsai and S.G. Weber, in preparation.
[16] W.J. Albery and M.L. Hitchman, *Ring-Disc Electrodes*, Clarendon Press, Oxford, 1971, p. 17.
[17] S.G. Weber and W.C. Purdy, *Anal. Chim. Acta*, 100 (1978) 531.
[18] D.W. Margerun, *Pure Appl. Chem.*, 55 (1983) 23.
[19] F.P. Bossu, K.L. Chellappa and D.W. Margerum, *J. Am. Chem. Soc.*, 99 (1977) 2195.
[20] M.P. Youngblood, K.L. Chellappa, C.E. Banniser and D.W. Margerum, *J. Am. Chem. Soc.*, 20 (1981) 1742.
[21] M.R. DeFelippis, C.P. Murthy, M. Faraggi and M.H. Klapper, *Biochemistry*, 28 (1989) 4847.
[22] S. Cheng, W.S. Craig, D. Mullen, Juerg. F. Tschopp, D. Dixon and M.D. Pierschbacher, *J. Med. Chem.*, 37 (1994) 1.
[23] B. Decock-Le Reverend, A. Lebkiri, C. Livera and L.D. Pettit, *Inorg. Chim. Acta.*, 124 (1986) L19.